



A Semi-analytical Method to Model Effective SINR Spatial Distribution in WiMAX Networks

Draft Version

Masood Maqbool, Marceau Coupechoux, Philippe Godlewski

Département Informatique et Réseaux

Institut TELECOM, TELECOM ParisTech

December 23, 2008

Contents

Contents	i
List of Acronyms	ii
1 Introduction	1
2 Network Dimensioning	1
2.1 Radio Coverage	2
2.2 Throughput Calculation	2
2.3 Traffic Analysis	4
3 Interference Model	4
3.1 Subcarrier SINR	4
3.2 Effective SINR	5
4 Simulator Details	5
4.1 Introduction	5
4.2 Wraparound Technique	6
4.3 Antenna Pattern	7
4.4 MS Spatial Distribution and Selection of Serving BS	9
4.5 Simulation Parameters	9
5 Semi-analytical Method	9
5.1 Simulations and Distribution/Curve Fitting	11
5.2 Off-line Application	12
6 Numerical Results	12
7 Conclusion	15

List of Acronyms

BS	Base Station
BW	Bandwidth
DL	Downlink
GEV	Generalized Extreme Value
MCS	Modulation and Coding Scheme
OFDM	Orthogonal Frequency Division Multiplex
OFDMA	Orthogonal Frequency Division Multiple Access
PDF	Probability Density Function
$SINR_{eff}$	Effective Signal to Noise-plus-Interference Ratio
TDD	Time Division Duplex
WiMAX	Worldwide Interoperability for Microwave Access

1 Introduction

In this report, we introduce a semi-analytical method to find out stationary probabilities of different MCS types for a mobile WiMAX network that can substitute a number of simulations. We start with Monte Carlo simulations and find out spatial distributions of Effective Signal to Noise-plus-Interference Ratio ($SINR_{eff}$) for some integral values of shadowing standard deviation σ_{SH} . It is shown that the probability density functions (PDFs) of $SINR_{eff}$ can be approximated by Generalized Extreme Value (GEV) distributions [1]. We exhibit that GEV distributions' parameters can be expressed in terms of σ_{SH} using polynomial. Instead of simulations, these polynomials can then be used to find out GEV distribution, and hence MCS probabilities, for any desired value of σ_{SH} in the above range. We further show that these polynomials can be used for other cell configurations with acceptable deviation and significant time saving.

Rest of the report is organized as follows: section 2 gives a brief description of network dimensioning study and relative details of IEEE 802.16e system. In section 3, $SINR_{eff}$ computation is discussed. Descriptive account of simulator can be found in section 4. The proposed semi-analytical method is explained by considering the frequency reuse type 3x3x3 in section 5 and numerical results are presented in section 6. The conclusion of the report has been discussed in section 7.

For explanation of semi-analytical method, only one frequency reuse type has been considered. However, method is equally applicable to five other possible reuse types: 1x1x1, 1x3x1, 1x3x3, 3x1x1 and 3x3x1 (cf. [2] for details on reuse types). The results pertaining to these five reuse types are listed down in the appendix of this report. The appendix also includes the results for reuse type 1x3x1 when beamforming is also considered. The semi-analytical method is described .

2 Network Dimensioning

The study of network dimensioning for mobile WiMAX networks can be divided into different components. As shown in Fig. 1, we classify it into three components: *Radio Coverage*, *Throughput Calculation* and *Traffic Analysis*. The work carried out in this paper focuses on *Radio Coverage* and *Throughput Calculation* blocks.

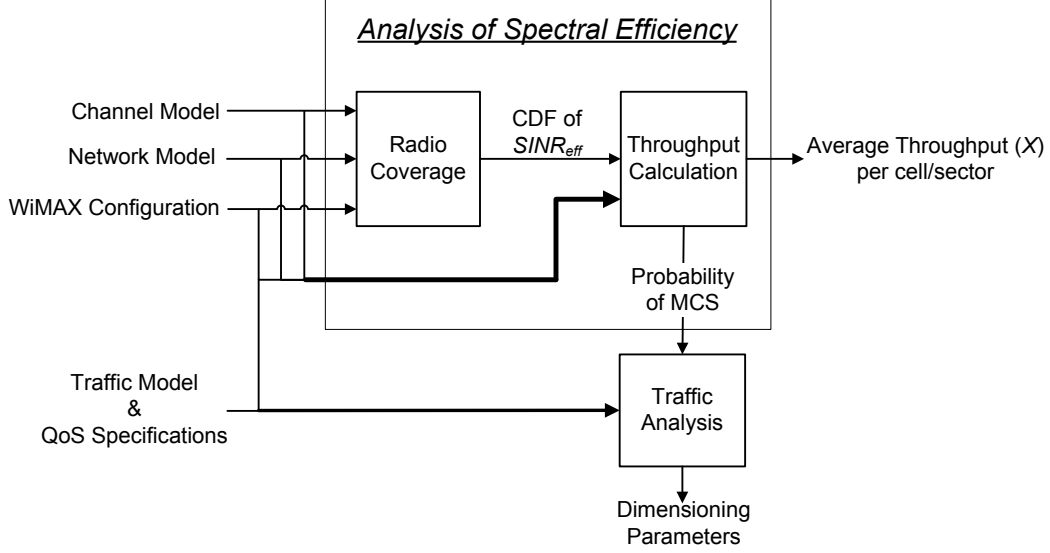


Figure 1: System overview.

2.1 Radio Coverage

The input parameters to this block are: channel model, network model and WiMAX configuration. These parameters are mainly based on [2]. The output of this block is CDF of $SINR_{eff}$ which can be obtained through Monte Carlo simulations. The disadvantage of simulation approach is excessive time consumption. In this report, we intend to substitute the simulation approach for a semi-analytical method.

We have considered distributed subcarrier permutation type PUSC in our simulations. The analysis equally holds for subcarrier permutation type FUSC. As mentioned earlier, the frequency reuse type 3x3x3 (see Fig. 2) is considered. To represent a reuse type, consider $N_c \times N_s \times N_f$ a generalized notation such that N_c represents the number of cells per cluster (see Fig. 2 for example), N_s is the number of sectors per cell and N_f gives the frequency reuse within a cell.

2.2 Throughput Calculation

Once the *Radio Coverage* block furnishes the CDF of $SINR_{eff}$, we require thresholds values of different MCS types to calculate MCS probabilities. Six different MCS types have been considered in our simulation model: QPSK-

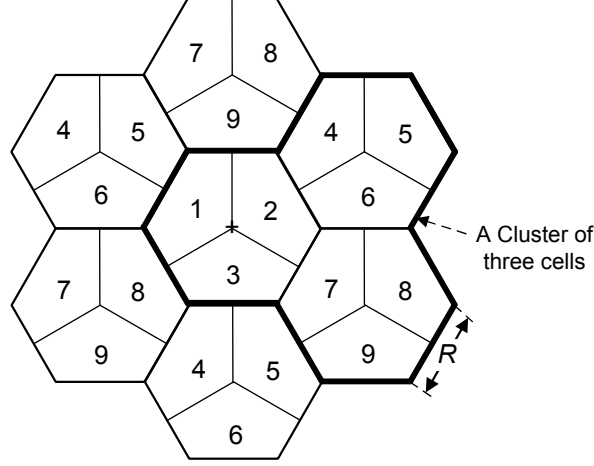


Figure 2: Frequency Reuse Pattern 3x3x3 (R is the cell range).

1/2 (the most robust), QPSK-3/4, 16QAM-1/2, 64QAM-2/3 and 64QAM-3/4 (for the best radio conditions). $SINR_{eff}$ threshold values for MCS types are given in Tab.1 and have been referred from [3]. If $SINR_{eff}$ of a mobile station (MS) is less than the threshold of the most robust MCS (i.e., less than 2.9 dB), it can neither receive nor transmit anything and is said to be in outage. We call outage as MCS type 0.

Using the probabilities of MCS, the average cell throughput X [bps] in DL is given as:

$$X = \frac{N_S}{T_F} \sum_{k=1}^K m_k p_k, \quad (1)$$

where K represents the total number of considered MCS types. The other two variables, p_k and m_k , are respectively the probability and bits per slot for MCS type k , N_S is the number of slots in DL sub-frame in a cell (i.e., per three sectors) and T_F is the duration of TDD (time division duplex) frame.

Total bandwidth in our simulator has been set to 10 MHz. The number of OFDM symbols in a WiMAX TDD frame is considered to be 47 [2]. We assume two symbols fixed for common channel transmissions. The rest of 45 symbols are partitioned between DL and UL sub-frames with DL part assuming two third of the symbols. Considering the symbol/bandwidth information, reuse type 3x3x3 and permutation type PUSC, there are $N_S = 450 \times 1/3$ slots in DL sub-frame, where 1/3 appears because of reuse type.

Table 1: Threshold of $SINR_{eff}$ values for six MCS types [3].

Index	MCS	bits per slot m_k	$SINR_{eff}$ [dB]
0	Outage	0	< 2.9
1	QPSK 1/2	48	2.9
2	QPSK 3/4	72	6.3
3	16QAM 1/2	96	8.6
4	16QAM 3/4	144	12.7
5	64QAM 2/3	192	16.9
6	64QAM 3/4	216	18

2.3 Traffic Analysis

From *Throughput Calculation*, we get the available sector/cell throughput. However, utilization of this throughput depends upon the scheduling of different types of incoming traffic. A number of traffic types, characterized by application and QoS specifications, are defined in [2]. Unsolicited grant service (UGS) and best effort (BE) are two examples of these traffic types.

To carry out traffic analysis, MCS probabilities are required from *Throughput Calculation* block. In [4] and [5], we have exhibited how the MCS probabilities are utilized in traffic analysis.

Before the semi-analytical method is presented, we discuss the interference model used in the simulations.

3 Interference Model

3.1 Subcarrier SINR

SINR of a subcarrier n is given as:

$$SINR_n = \frac{P_{n,Tx} a_{n,Sh}^{(0)} a_{n,FF}^{(0)} \frac{K}{d^{(0)\alpha}}}{N_0 W_{Sc} + \sum_{b=1}^B P_{n,Tx} a_{n,Sh}^{(b)} a_{n,FF}^{(b)} \frac{K}{d^{(b)\alpha}}}, \quad (2)$$

where $P_{n,Tx}$ is the per subcarrier power, $a_{n,Sh}^{(0)}$ and $a_{n,FF}^{(0)}$ represent the shadowing (log-normal) and fast fading (Rician) factors for the signal received from serving BS respectively, B is the number of interfering BS, K is the path loss

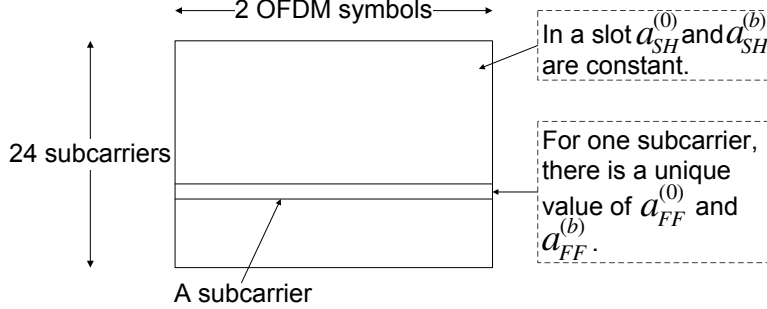


Figure 3: Shadowing and fast fading over a PUSC slot.

constant, α is the path loss exponent and $d^{(0)}$ is the distance between MS and serving BS. The terms with superscript b are related to interfering BS. W_{sc} is the subcarrier frequency spacing and N_0 is the thermal noise density. The values of pathloss constant and exponent are derived from COST231 Hata macro-urban path loss model [2].

3.2 Effective SINR

We compute $SINR_{eff}$ over the subcarriers of a slot. The physical abstraction model used for this purpose is mean instantaneous capacity (MIC) [2]. For computation of $SINR_{eff}$, log-normal shadowing is drawn randomly for a slot and is same for all subcarriers of a slot. Since subcarriers of a subchannel (hence a slot) are not contiguous, fast fading is drawn independently for every subcarrier of a slot (Fig. 3). For fast fading, Rayleigh distribution has been considered in simulations.

4 Simulator Details

4.1 Introduction

In this section details about simulation of WiMAX network are given. Wrap-around technique, spatial distribution of MS, sectorization, antenna diagram, etc, have been described. The parameter values used in simulations are also given. Monte Carlo simulations are carried (for subcarrier distributions PUSC) and simulation results are compared for different types of reuse patterns. It is to be noted that simulations are carried out in DL direction only

and hence all the information in this section is customized accordingly.

4.2 Wraparound Technique

This text on wraparound method is based on [6] and [7]. We start with introduction of few terms. The symmetry in a hexagonal network means that one would not notice the difference when standing in the middle of the hexagon, while the hexagon is rotated or reflected accordingly. In a two tier network with finite number of nodes, only the central cell enjoys such symmetry. In such a network only the data collected in the central cell will have statistical characteristics equivalent to a network consisting of infinite cells. Also to collect a large amount of data, it is desired to drop the MS in the cells other than the central one. To address this issue, idea of wraparound is introduced.

Using wraparound method, the network is extended to a cluster of network consisting of eight copies of the original hexagonal network. With the original hexagonal network in the middle, eight copies are attached to it symmetrically as shown in the Fig. 4. This cell layout is wraparound to form a toroidal surface. In order to be able to perform this mapping, the number of cells in a cluster has to be a rhombic number. There is a one-to-one mapping between cells/sectors of the center hexagon and cells/sectors of each copy. In this way every cell in the extended network is identified with one of the cells in the central original network. Those corresponding cells have thus the same antenna configuration, traffic, fading, etc, except the location. This correspondence is shown in Fig. 4 through shaded sectors of the same cell in all the networks.

Let us consider a two tier wraparound model. The signal or interference from any MS to a given cell is treated as if that MS is in the first 2 rings of neighboring cells. The distance from any MS to any BS is obtained as follows. A coordinate system is defined with center cell of original network at $(0, 0)$. The path distance and angle used to compute the path loss and antenna gain of a MS at (x, y) to a BS at (a, b) is the minimum of the following:

$$\text{Distance1} = \text{Distance between } (x, y) \text{ and } (a, b)$$

$$\text{Distance2} = \text{Distance between } (x, y) \text{ and } (a + 2.5\sqrt{3}D, b + D/2)$$

$$\text{Distance3} = \text{Distance between } (x, y) \text{ and } (a + \sqrt{3}D, b + 4D)$$

Distance4 = Distance between (x, y) and $(a - \sqrt{3}D/2, b + 7.5D)$

Distance5 = Distance between (x, y) and $(a - 1.5\sqrt{3}D, b + 3.5D)$

Distance6 = Distance between (x, y) and $(a - 2.5\sqrt{3}D, b - D/2)$

Distance7 = Distance between (x, y) and $(a - \sqrt{3}D, b - 4D)$

Distance8 = Distance between (x, y) and $(a + \sqrt{3}D/2, b - 7.5D)$

Distance9 = Distance between (x, y) and $(a + 1.5\sqrt{3}D, b - 3.5D)$

where D is the distance between two neighboring BS.

4.3 Antenna Pattern

Antenna pattern for simulations has been referred from [2]. According to [2], all BS antenna elements have the beam pattern defined by 3GPP2. It is given by the formula:

$$G(\psi) = G_{max} + \max \left[-12 \left(\frac{\psi}{\psi_{3dB}} \right)^2, -G_{FB} \right]$$

where

G_{max} in (dBi) is the maximum antenna gain (i.e. in the boresight direction).

ψ is the angle (in degrees) of arrival relative to boresight with $|\psi| \leq 180$.

ψ_{3dB} is the 3dB beam width (in degrees). It equals 70° in 3GPP antenna pattern [2].

G_{FB} is the front-to-back ratio in dBi (=25 dBi [2]). $G_{FB}=0$ for omni-directional antennas.

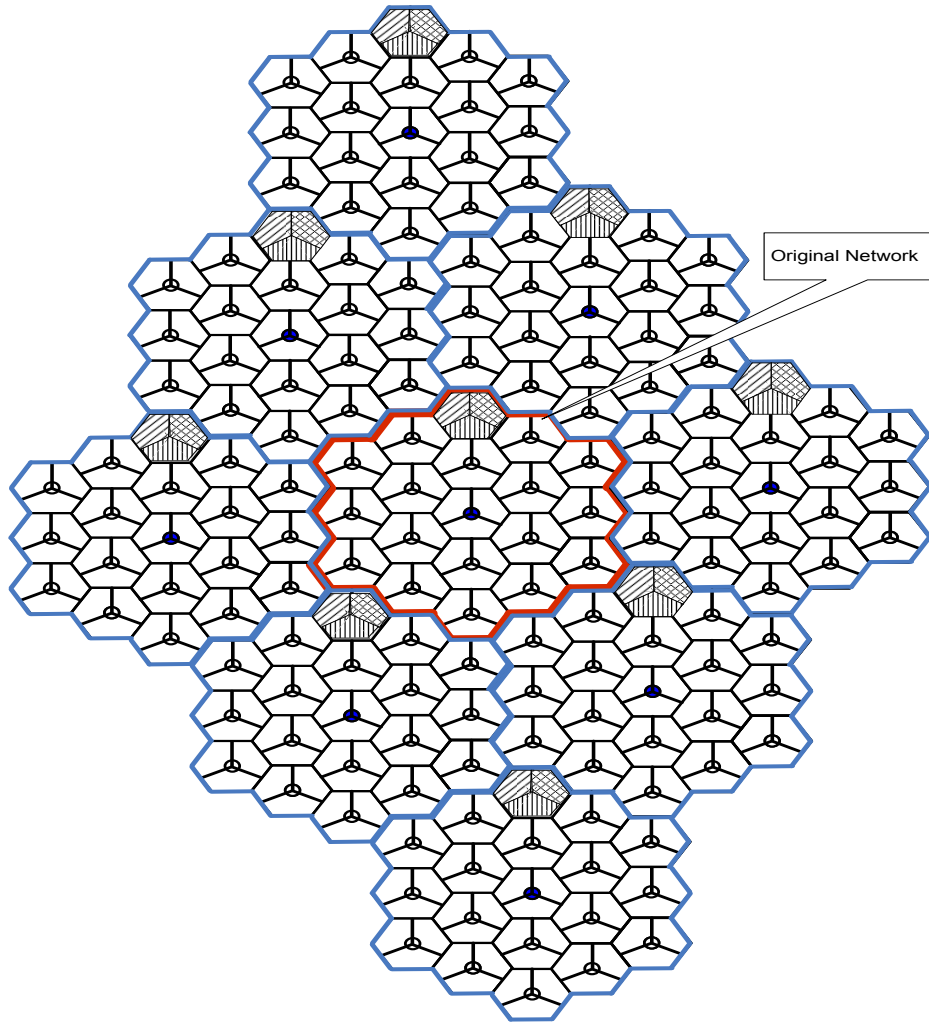


Figure 4: An example of wraparound network.

4.4 MS Spatial Distribution and Selection of Serving BS

MS is dropped into the cell using uniform random distribution. There are total three MS dropped into a cell. If the cell is sectorized, each sector has exactly one MS. Since we are using wraparound technique, three MS are dropped into every cell of the network.

There are two ways by which a MS can attach itself to a BS: minimum distance or best link. Since best link is more close to practical scenario, it is being employed in the simulations. For each MS, signal strength is measured from all the cells/sectors in the network. The MS selects the cell/sector from which it receives the maximum signal strength. The rest of the cells/sectors are the interfering ones (depending on the reuse pattern). Shadowing effect is taken into account during this procedure. However, fast fading is not considered during serving BS selection. The reason being that MS measures the signal from BS over sufficient interval of time to average out the fading effect.

4.5 Simulation Parameters

Simulation parameters are listed in Tab-2. These values are mainly based on [2]. P_{Tx} of Tab-2 is the power transmitted by BS on all used subcarriers (data+pilot) in a cell. Power transmitted on one subcarrier is given by following expression:

$$P_{n,Tx} = \begin{cases} \frac{P_{Tx}N_f}{N_sN_{Sc}} & \text{for sectorized cells;} \\ \frac{P_{Tx}N_c}{N_sN_{Sc}} & \text{for non-sectorized cells;} \end{cases} \quad (3)$$

where N_c , N_f and N_s define the reuse type and N_{Sc} is the number of used subcarriers for a given bandwidth and subcarrier permutation type. It is clear from the above expression that subcarrier power may be different for all reuse patterns.

5 Semi-analytical Method

A systematic overview of the proposed semi-analytical method is depicted in Fig. 5. The method is divided into two steps: A) Simulations and Distribu-

Parameter	Value
Reuse type	3x3x3
No. of interfering BS	18
Carrier frequency f	2.5 GHz
Total rms transmit power of a cell P_{Tx}	43 dBm
Pathloss model $\frac{K}{d^\alpha}$	COST-HATA-231, $\alpha=3.5$, $K=1.4 \times 10^4$
Number of OFDMA symbol in a frame	47
Number of DL data OFDMA symbols	30
DL to UL OFDMA symbols' ratio	2:1
Network bandwidth	10MHz
Total number of available subcarriers	1024
Total number of used subcarriers (data+pilot) N_{Sc}	841
Subcarrier spacing Δf	10.9375 kHz
TDD Frame Duration	5 ms
Thermal noise density N_0	-174 dBm/Hz
One side of hexagonal cell R	1Km
Height of BS h_{BS}	32 m
Height of MS h_{MS}	1.5 m
Antenna Gain (boresight) G_{max}	16 dBi
3dB antenna beam width ψ_{3dB}	70°
Front-to-back antenna power ratio G_{FB}	25dBi

Table 2: Description and values of parameters used in simulations.

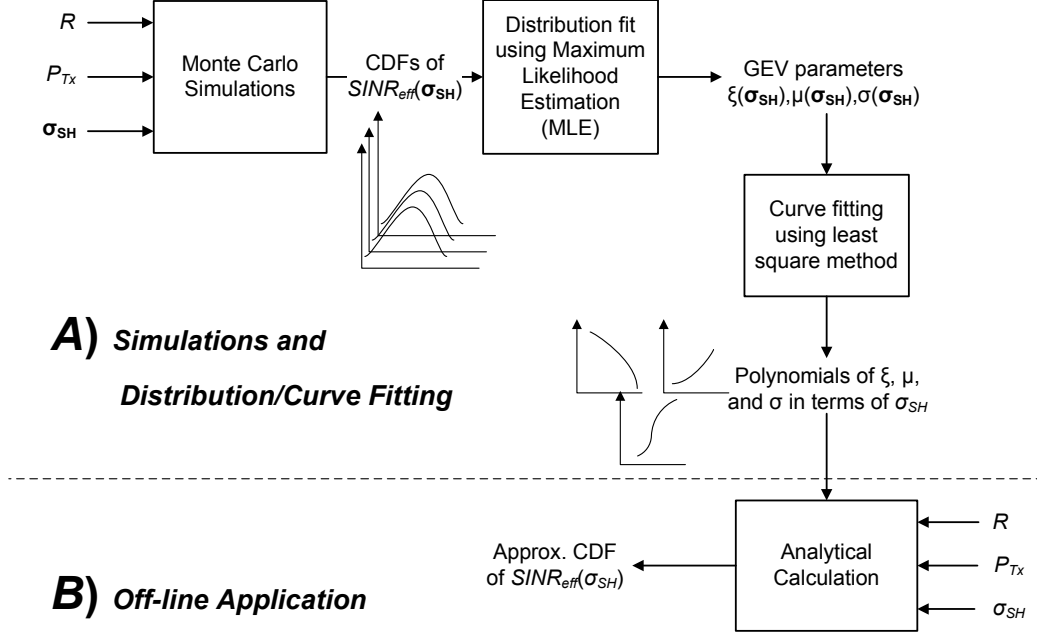


Figure 5: Overview of proposed semi-analytical method.

tion/Curve Fitting and B) Off-line Application. In the following text, these steps are explained in detail.

5.1 Simulations and Distribution/Curve Fitting

During this step, spatial distributions of $SINR_{eff}$ is obtained using Monte Carlo simulations for a given value of R , P_{Tx} and a specified range of σ_{SH} integral values.

Each distribution of $SINR_{eff}$ is specific to a value of σ_{SH} . With the help of distribution fit (based on maximum likelihood estimation), the parameters of GEV distribution (shape parameter ξ , scale parameter σ and location parameter μ), approximating the simulation PDFs, are acquired for each value of σ_{SH} .

In order to evaluate the distribution fit, the dissimilarity or error Ξ between GEV and simulation PDFs, φ_{GEV} and φ_{sim} , is quantified as follows[8]:

$$\Xi \triangleq \int_{-\infty}^{\infty} |\varphi_{GEV}(t) - \varphi_{sim}(t)| dt. \quad (4)$$

Since the area under a PDF is 1, the maximum value of error can be 2. Hence the value of error can be between 0 and 2 i.e., $0 \leq \Xi \leq 2$.

Once it is verified that simulation PDFs of $SINR_{eff}$ can be approximated by GEV PDFs, three GEV parameters are then separately plotted against the integral values of σ_{SH} . With the help of curve fitting (using least square method), distinct polynomials, expressing each parameter in terms of σ_{SH} , are found.

5.2 Off-line Application

To calculate $SINR_{eff}$ distribution for any desired value (integral/non-integral) of σ_{SH} in the range specified in section 5.1, we no longer require to carry out time consuming Monte Carlo simulations. It is sufficient to find out GEV parameters through polynomials for that value of σ_{SH} . Then using GEV CDF and thresholds values of $SINR_{eff}$ for different MCS types of Tab. 1, probabilities of these MCS can be obtained. These MCS probabilities are used to calculate sector/cell throughput by applying Eq. 1. In section 6, we also show that results obtained through this method are applicable for various values of R and P_{Tx} .

6 Numerical Results

In this section, we present the numerical results. For Monte Carlo simulations, range of σ_{SH} is considered to be 4, 5, ..., 12. Other input parameters are $R = 1500$ m and $P_{Tx} = 43$ dBm. An $SINR_{eff}$ distribution is obtained for each value of σ_{SH} . Using distribution fitting, GEV parameters are determined for each of these distributions. As an example, in Fig. 6, approximation of $SINR_{eff}$ PDF (obtained through simulation) by a GEV PDF for $\sigma_{SH} = 9$ dB is shown. As can be noticed, the two distributions only have a dissimilarity error of 0.052 which is 2.6% of the maximum possible error.

GEV parameters, obtained through distribution fitting, are separately plotted against σ_{SH} values in Figs. 7, 8 and 9. With the help of curve fitting, polynomials of the curves approximating these plots are found and are also given in the figures.

To validate off-line application (cf. section 5.2), we choose an arbitrary value $\sigma_{SH} = 7.5$ dB. We calculate the GEV parameters through polynomials and get PDF, MCS probabilities and cell throughput. For the same value

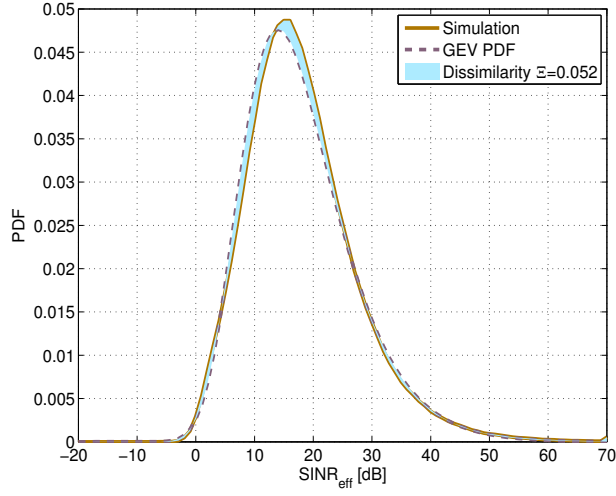


Figure 6: $SINR_{eff}$ distribution through simulation and GEV polynomial for $\sigma_{SH} = 9$ dB, $R = 1500$ m, $P_{Tx} = 43$ dBm and reuse 3x3x3.

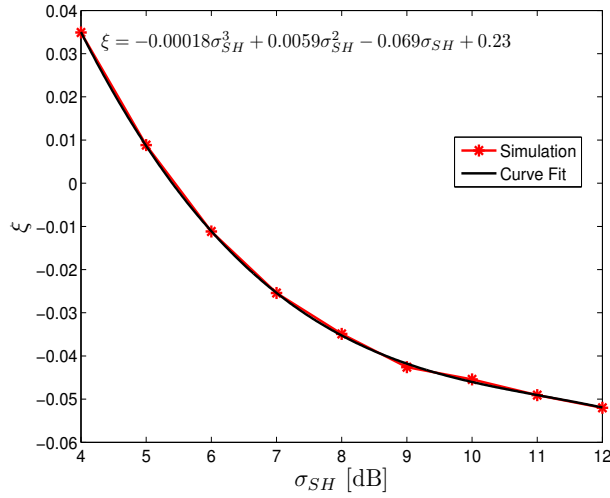


Figure 7: Shape parameter ξ of GEV distribution versus σ_{SH} for $R = 1500$ m, $P_{Tx} = 43$ dBm and reuse 3x3x3.

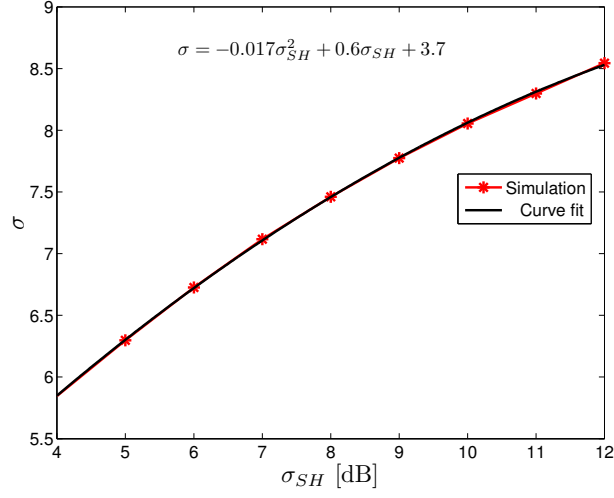


Figure 8: Scale parameter σ of GEV distribution versus σ_{SH} for $R = 1500$ m, $P_{Tx} = 43$ dBm and reuse 3x3x3.

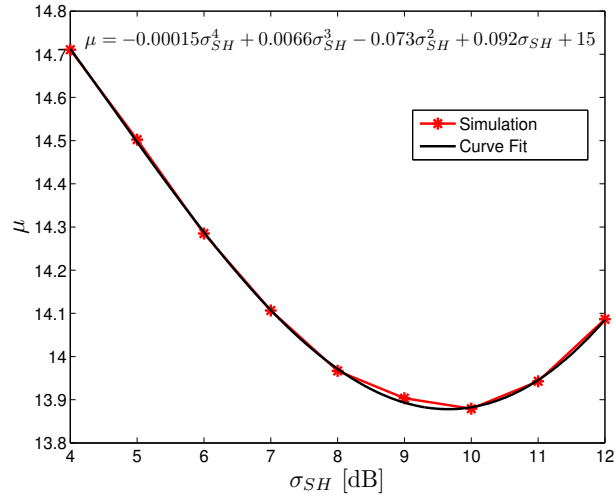


Figure 9: Location parameter μ of GEV distribution versus σ_{SH} for $R = 1500$ m, $P_{Tx} = 43$ dBm and reuse 3x3x3.

of σ_{SH} and assuming the values of $R = 1500$ m, $P_{Tx} = 43$ dBm, we find the PDFs, MCS probabilities and cell throughput through simulations. Furthermore, we also check the applicability of results obtained through GEV parameters, with $\sigma_{SH} = 7.5$ dB, for various cell configurations. For this purpose, we fix $\sigma_{SH} = 7.5$ dB and carry out simulations for different values of R and P_{Tx} . The maximum value of R is considered to be 2000 m beyond which outage probability increases rapidly [9]. PDFs, MCS probabilities and average cell throughput are obtained through simulations with different configurations are compared with those obtained through GEV parameters.

The results of validation and applicability for various cell configurations are given in Fig. 10 and Tab. 3. For MCS probabilities, maximum difference was found to be 0.06 (for MCS 64QAM-3/4) with simulation configuration of $R = 1000$ m, $P_{Tx} = 43$ dBm, which is 13% of the value of MCS 64QAM-3/4 probability. As far as cell throughput and PDF error are concerned, the percentage error w.r.t maximum possible error never exceeds 5% and cell throughput does not differ more than 5.47% for all cell configurations.

The simulations were run on a computer with following specifications: 3 GHz Intel Core 2 Duo processor, 2 GB RAM and 4 MB shared L2 cache. Time taken by one Monte Carlo simulation was about 5 hours. Time required for semi-analytical method is around $N_{SH} \times 5$ hours, where N_{SH} is the length of vector σ_{SH} . If MCS distributions are required for N different scenarios (each defined by specific values of σ_{SH} , R and P_{Tx}), our proposed method always requires fixed duration which is equal to $N_{SH} \times 5$ hours while the same task carried out by Monte Carlo simulations will require $N \times 5$ hours.

7 Conclusion

In this report we have detailed the validation of mono/multi-profile BE traffic models for WiMAX network. Results through and analytical model are in good agreement. Apart from validation, we have also shown how robust the analytical model is w.r.t. changes in various assumptions. In robustness study, different traffic distributions, radio channel with memory and different load conditions were considered. For the case of traffic distributions, results were compared for exponential and pareto (low/high cut off) distributions. Radio channels with memory and with no memory were considered. Results were also good for low, medium and high traffic loads.

Table 3: Comparison of results obtained through simulation and GEV parameters for $\sigma_{SH} = 7.5$ dB for reuse 3x3x3.

Simulation Configuration		Dissimilarity Ξ	Percentage w.r.t max error	Throughput X [Mbps]		Percentage difference
P_{Tx} [dBm]	R [m]			Sim	GEV	
43	1000	0.095	4.73	5	4.73	5.47
43	1250	0.073	3.65	4.96	4.73	4.57
43	1500	0.056	2.83	4.88	4.73	3.17
43	1750	0.058	2.92	4.78	4.73	1.18
43	2000	0.1	5	4.66	4.73	1.35
40	1500	0.065	3.27	4.75	4.73	0.49
46	1500	0.075	3.77	4.96	4.73	4.72

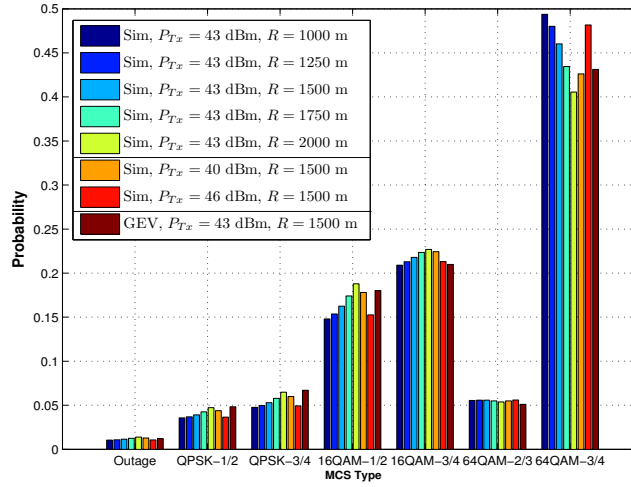


Figure 10: MCS Probabilities for $\sigma_{SH} = 7.5$ dB and reuse 3x3x3.

Appendices

Reuse Type 1x1x1

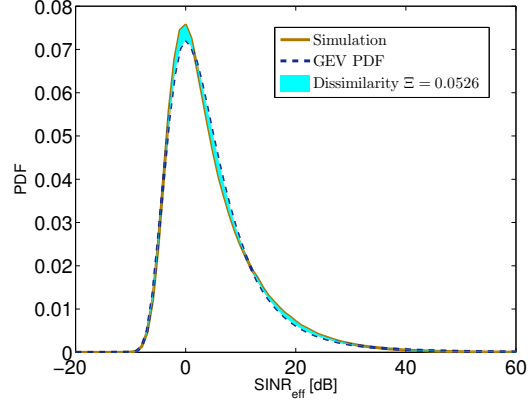


Figure 11: $SINR_{eff}$ distribution through simulation and GEV polynomial for $\sigma_{SH} = 9$ dB, $R = 1500$ m, $P_{Tx} = 43$ dBm and reuse 1x1x1.

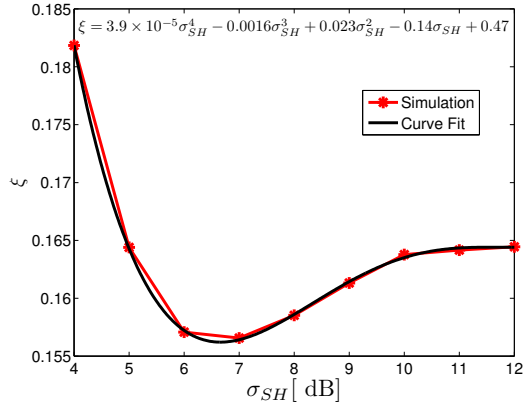


Figure 12: Shape parameter ξ of GEV distribution versus σ_{SH} for $R = 1500$ m, $P_{Tx} = 43$ dBm and reuse 1x1x1.

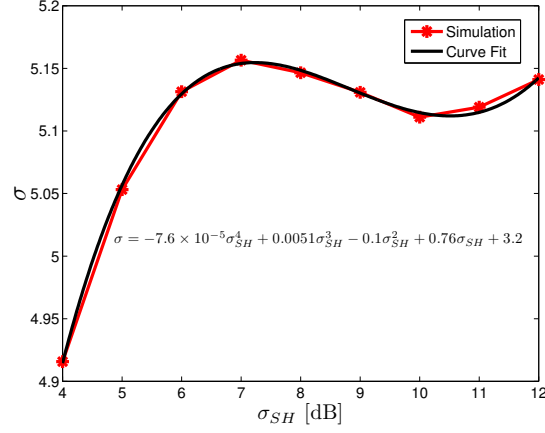


Figure 13: Scale parameter σ of GEV distribution versus σ_{SH} for $R = 1500$ m, $P_{Tx} = 43$ dBm and reuse 1x1x1.

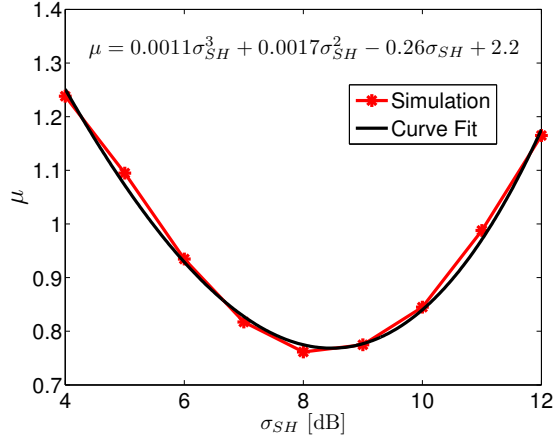


Figure 14: Location parameter μ of GEV distribution versus σ_{SH} for $R = 1500$ m, $P_{Tx} = 43$ dBm and reuse 1x1x1.

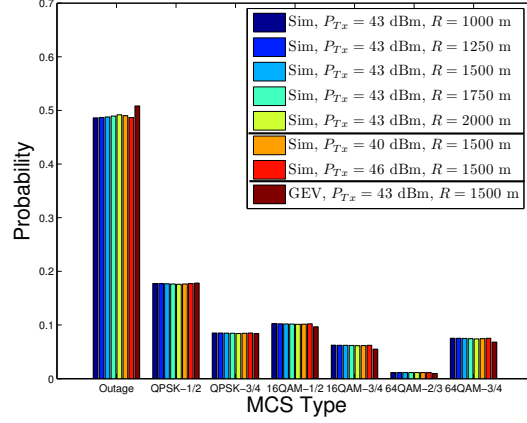


Figure 15: MCS Probabilities for $\sigma_{SH} = 7.5$ dB and reuse 1x1x1.

Table 4: Comparison of results obtained through simulation and GEV parameters for $\sigma_{SH} = 7.5$ dB for reuse 1x1x1.

Simulation Configuration		Dissimilarity Ξ	Percentage w.r.t max error	Throughput X [Mbps]		Percentage difference
P_{Tx} [dBm]	R [m]			Sim	GEV	
43	1000	0.05	2.50	4.67	4.35	6.79
43	1250	0.05	2.50	4.66	4.35	6.65
43	1500	0.05	2.50	4.65	4.35	6.42
43	1750	0.05	2.53	4.64	4.35	6.08
43	2000	0.05	2.57	4.61	4.35	5.59
40	1500	0.05	2.54	4.63	4.35	5.95
46	1500	0.05	2.50	4.66	4.35	6.66

Reuse Type 1x3x1

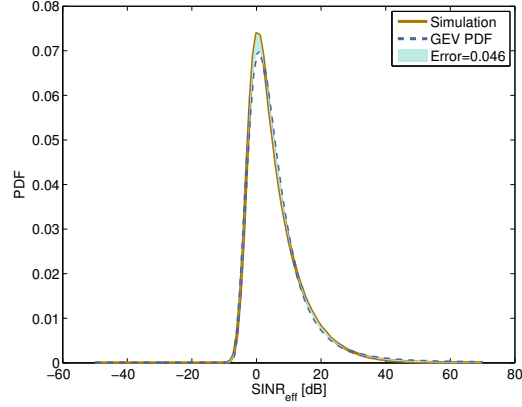


Figure 16: $SINR_{eff}$ distribution through simulation and GEV polynomial for $\sigma_{SH} = 9$ dB, $R = 1500$ m, $P_{Tx} = 43$ dBm and reuse 1x3x1.

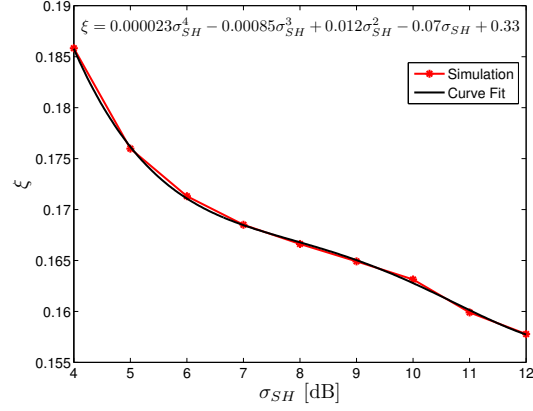


Figure 17: Shape parameter ξ of GEV distribution versus σ_{SH} for $R = 1500$ m, $P_{Tx} = 43$ dBm and reuse 1x3x1.

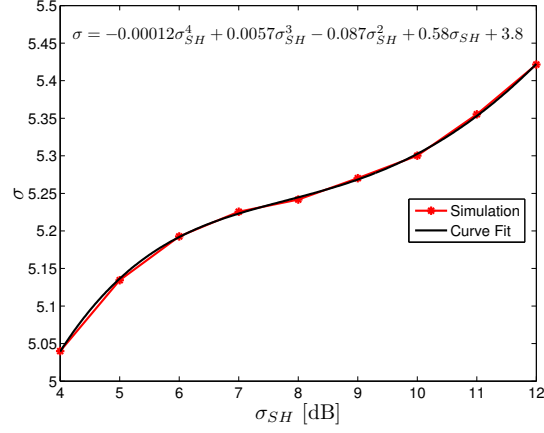


Figure 18: Scale parameter σ of GEV distribution versus σ_{SH} for $R = 1500$ m, $P_{Tx} = 43$ dBm and reuse 1x3x1.

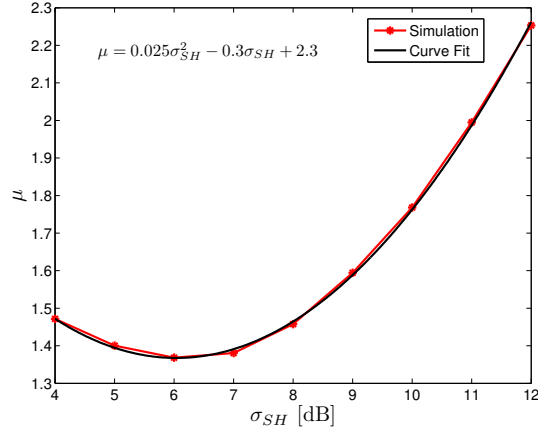


Figure 19: Location parameter μ of GEV distribution versus σ_{SH} for $R = 1500$ m, $P_{Tx} = 43$ dBm and reuse 1x3x1.

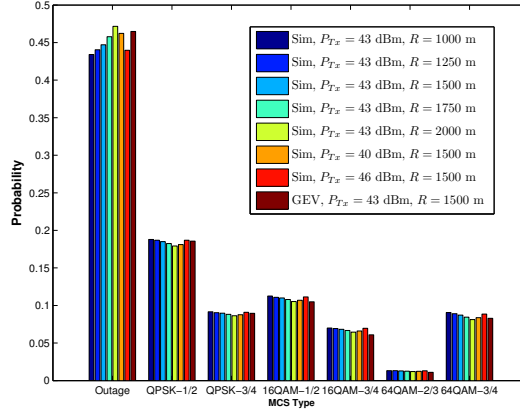


Figure 20: MCS Probabilities for $\sigma_{SH} = 7.5$ dB and reuse 1x3x1.

Table 5: Comparison of results obtained through simulation and GEV parameters for $\sigma_{SH} = 7.5$ dB for reuse 1x3x1.

Simulation Configuration		Dissimilarity Ξ	Percent-age w.r.t max error	Throughput X [Mbps]		Percent-age difference
P_{Tx} [dBm]	R [m]			Sim	GEV	
43	1000	0.056	2.80	15.82	14.65	7.42
43	1250	0.054	2.70	15.62	14.65	6.23
43	1500	0.053	2.65	15.39	14.65	4.84
43	1750	0.064	3.20	15.04	14.65	2.62
43	2000	0.085	4.25	14.59	14.65	0.37
40	1500	0.071	3.55	14.92	14.65	1.80
46	1500	0.054	2.70	15.62	14.65	6.24

Reuse Type 1x3x3

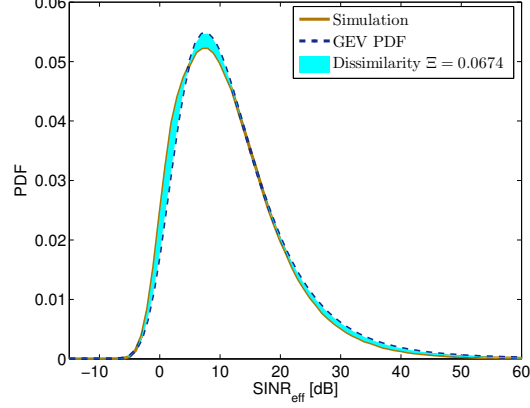


Figure 21: $SINR_{eff}$ distribution through simulation and GEV polynomial for $\sigma_{SH} = 9$ dB, $R = 1500$ m, $P_{Tx} = 43$ dBm and reuse 1x3x3.

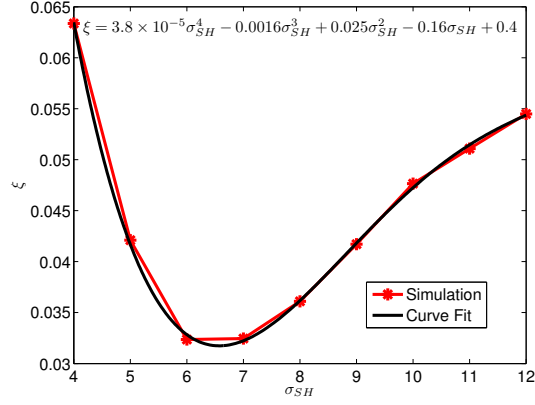


Figure 22: Shape parameter ξ of GEV distribution versus σ_{SH} for $R = 1500$ m, $P_{Tx} = 43$ dBm and reuse 1x3x3.

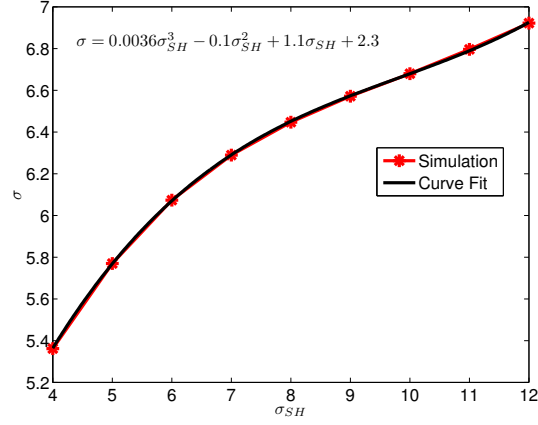


Figure 23: Scale parameter σ of GEV distribution versus σ_{SH} for $R = 1500$ m, $P_{Tx} = 43$ dBm and reuse 1x3x3.

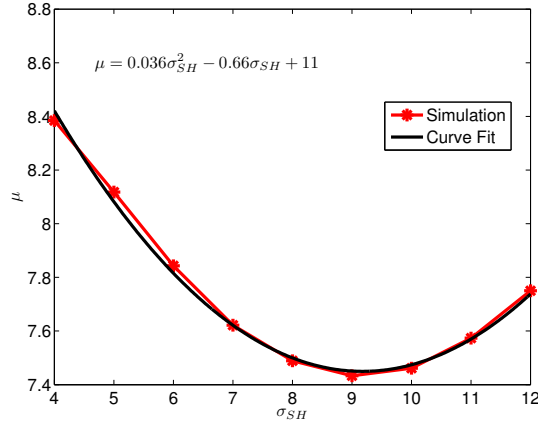


Figure 24: Location parameter μ of GEV distribution versus σ_{SH} for $R = 1500$ m, $P_{Tx} = 43$ dBm and reuse 1x3x3.

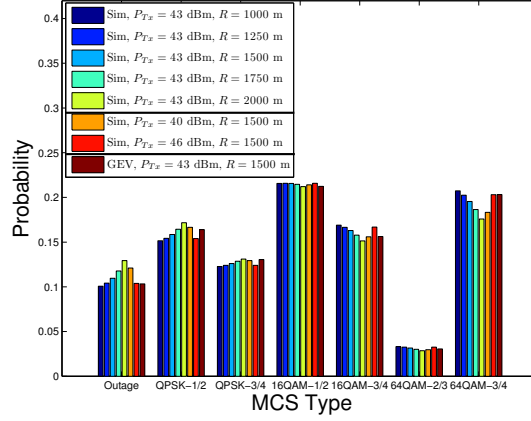


Figure 25: MCS Probabilities for $\sigma_{SH} = 7.5$ dB and reuse 1x3x3.

Table 6: Comparison of results obtained through simulation and GEV parameters for $\sigma_{SH} = 7.5$ dB for reuse 1x3x3.

Simulation Configuration		Dissimilarity Ξ	Percentage w.r.t max error	Throughput X [Mbps]		Percentage difference
P_{Tx} [dBm]	R [m]			Sim	GEV	
43	1000	0.05	2.45	10.11	9.89	2.14
43	1250	0.05	2.48	9.99	9.89	1.04
43	1500	0.06	2.93	9.82	9.89	0.69
43	1750	0.09	4.26	9.59	9.89	3.14
43	2000	0.13	6.29	9.30	9.89	6.39
40	1500	0.10	4.82	9.51	9.89	4.05
46	1500	0.05	2.47	10.0	9.89	1.14

Reuse Type 3x1x1

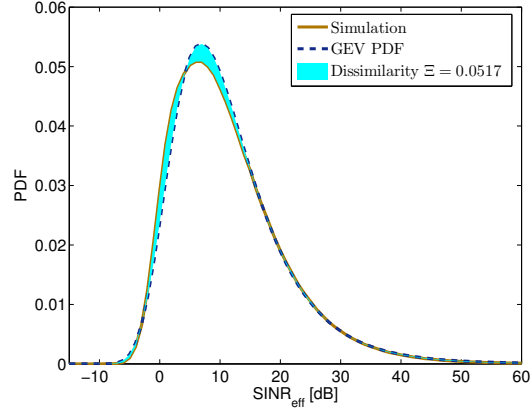


Figure 26: $SINR_{eff}$ distribution through simulation and GEV polynomial for $\sigma_{SH} = 9$ dB, $R = 1500$ m, $P_{Tx} = 43$ dBm and reuse 3x1x1.

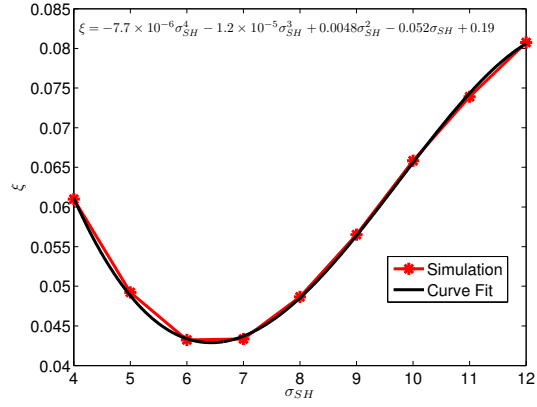


Figure 27: Shape parameter ξ of GEV distribution versus σ_{SH} for $R = 1500$ m, $P_{Tx} = 43$ dBm and reuse 3x1x1.

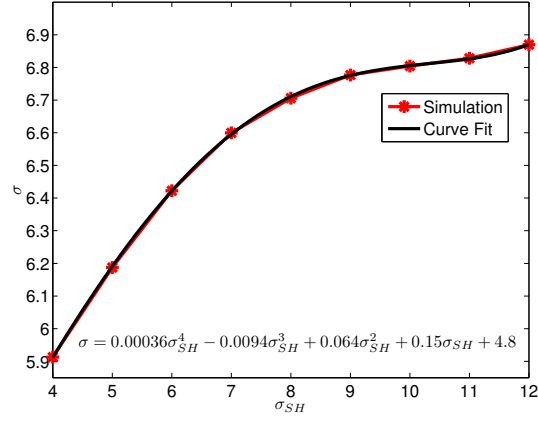


Figure 28: Scale parameter σ of GEV distribution versus σ_{SH} for $R = 1500$ m, $P_{Tx} = 43$ dBm and reuse 3x1x1.

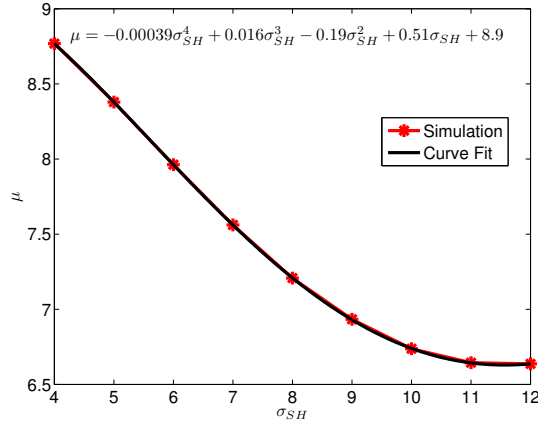


Figure 29: Location parameter μ of GEV distribution versus σ_{SH} for $R = 1500$ m, $P_{Tx} = 43$ dBm and reuse 3x1x1.

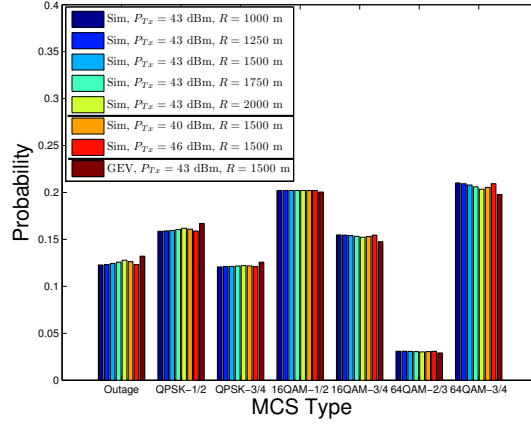


Figure 30: MCS Probabilities for $\sigma_{SH} = 7.5$ dB and reuse 3x1x1.

Table 7: Comparison of results obtained through simulation and GEV parameters for $\sigma_{SH} = 7.5$ dB for reuse 3x1x1.

Simulation Configuration		Dissimilarity Ξ	Percentage w.r.t max error	Throughput X [Mbps]		Percentage difference
P_{Tx} [dBm]	R [m]			Sim	GEV	
43	1000	0.03	1.46	3.28	3.18	3.14
43	1250	0.03	1.47	3.27	3.18	2.96
43	1500	0.03	1.55	3.26	3.18	2.68
43	1750	0.03	1.71	3.25	3.18	2.25
43	2000	0.04	1.97	3.23	3.18	1.65
40	1500	0.04	1.78	3.24	3.18	2.08
46	1500	0.03	1.47	3.27	3.18	2.98

Reuse Type 3x3x1

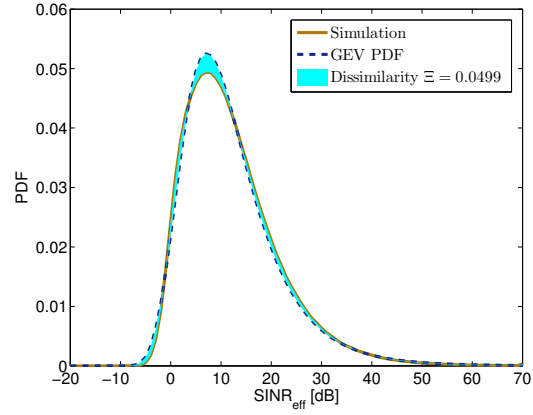


Figure 31: $SINR_{eff}$ distribution through simulation and GEV polynomial for $\sigma_{SH} = 9$ dB, $R = 1500$ m, $P_{Tx} = 43$ dBm and reuse 3x3x1.

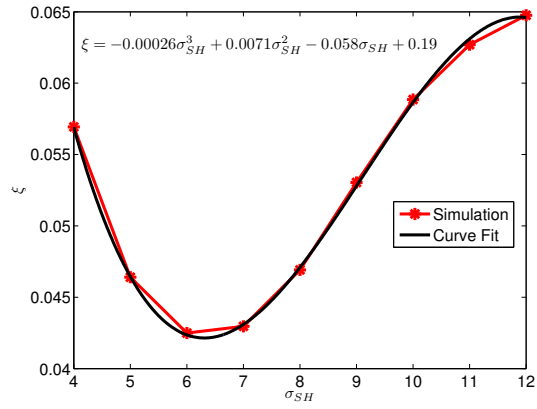


Figure 32: Shape parameter ξ of GEV distribution versus σ_{SH} for $R = 1500$ m, $P_{Tx} = 43$ dBm and reuse 3x3x1.

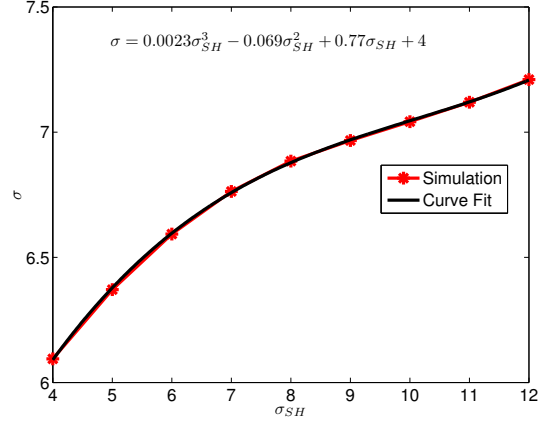


Figure 33: Scale parameter σ of GEV distribution versus σ_{SH} for $R = 1500$ m, $P_{Tx} = 43$ dBm and reuse 3x3x1.

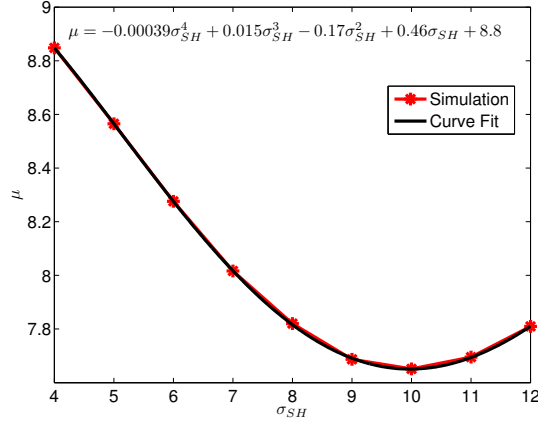


Figure 34: Location parameter μ of GEV distribution versus σ_{SH} for $R = 1500$ m, $P_{Tx} = 43$ dBm and reuse 3x3x1.

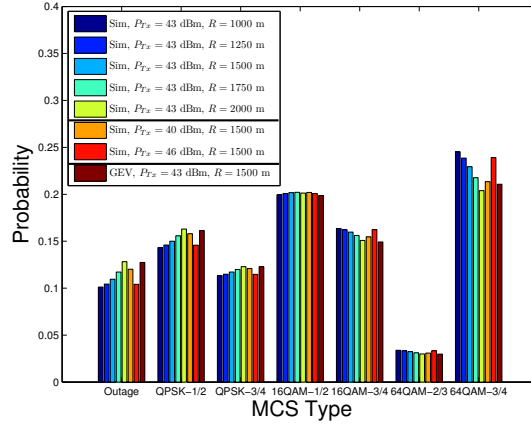


Figure 35: MCS Probabilities for $\sigma_{SH} = 7.5$ dB and reuse 3x3x1.

Table 8: Comparison of results obtained through simulation and GEV parameters for $\sigma_{SH} = 7.5$ dB for reuse 3x3x1.

Simulation Configuration		Dissimilarity Ξ	Percentage w.r.t max error	Throughput X [Mbps]		Percentage difference
P_{Tx} [dBm]	R [m]			Sim	GEV	
43	1000	0.07	3.28	10.55	9.76	7.53
43	1250	0.05	2.62	10.42	9.76	6.41
43	1500	0.04	1.77	10.24	9.76	4.73
43	1750	0.03	1.42	9.99	9.76	2.34
43	2000	0.06	3.03	9.67	9.76	0.83
40	1500	0.04	1.80	9.90	9.76	1.46
46	1500	0.05	2.67	10.43	9.76	6.51

Reuse Type 1x3x1 with Beamforming

The simulator details for a beamforming capable WiMAX network can be found in [10].

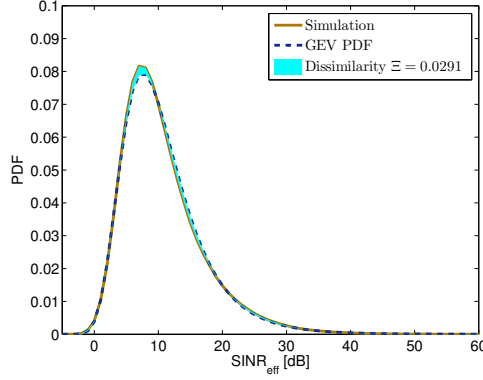


Figure 36: $SINR_{eff}$ distribution through simulation and GEV polynomial for $\sigma_{SH} = 9$ dB, $R = 1500$ m, $P_{Tx} = 43$ dBm and reuse 1x3x1 while taking into account beamforming.

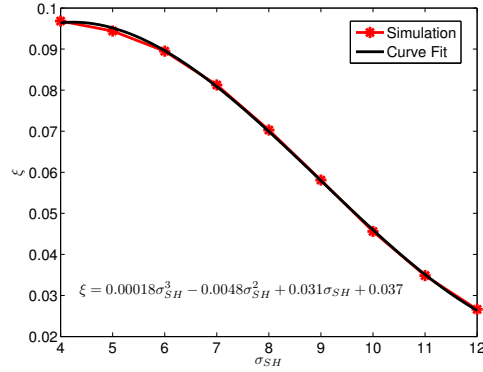


Figure 37: Shape parameter ξ of GEV distribution versus σ_{SH} for $R = 1500$ m, $P_{Tx} = 43$ dBm and reuse 1x3x1 while taking into account beamforming.

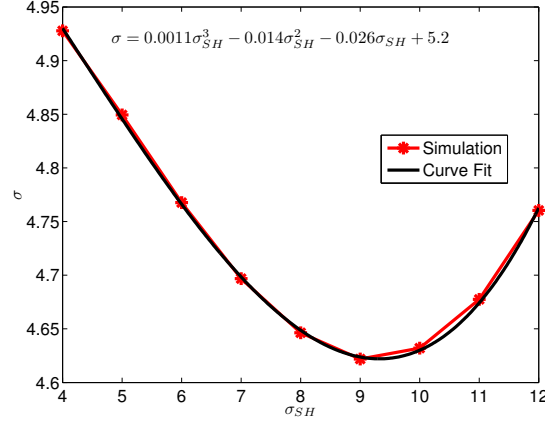


Figure 38: Scale parameter σ of GEV distribution versus σ_{SH} for $R = 1500$ m, $P_{Tx} = 43$ dBm and reuse 1x3x1 while taking into account beamforming.

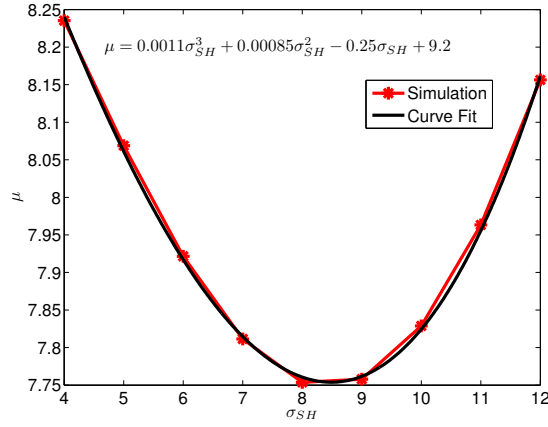


Figure 39: Location parameter μ of GEV distribution versus σ_{SH} for $R = 1500$ m, $P_{Tx} = 43$ dBm and reuse 1x3x1 while taking into account beamforming.

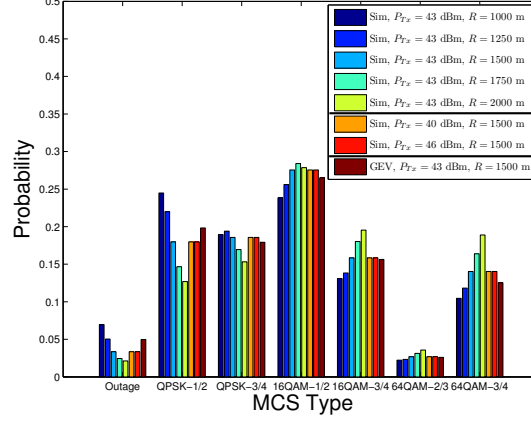


Figure 40: MCS Probabilities for $\sigma_{SH} = 7.5$ dB and reuse 1x3x1 while taking into account beamforming.

Table 9: Comparison of results obtained through simulation and GEV parameters for $\sigma_{SH} = 7.5$ dB for reuse 1x3x1 with beamforming.

Simulation Configuration		Dissimilarity Ξ	Percent-age w.r.t max error	Throughput X [Mbps]		Percent-age difference
P_{Tx} [dBm]	R [m]			Sim	GEV	
43	1000	0.23	11.60	25.38	27.66	9.00
43	1250	0.15	7.60	26.73	27.66	3.47
43	1500	0.04	2.01	28.81	27.66	4.00
43	1750	0.10	4.92	30.75	27.66	10.03
43	2000	0.19	9.31	32.31	27.66	14.39
40	1500	0.04	2.01	28.81	27.66	3.99
46	1500	0.04	2.01	28.82	27.66	4.00

References

- [1] S. Markose and A. Alentorn, “The Generalized Extreme Value (GEV) Distribution, Implied Tail Index and Option Pricing,” University of Essex, Department of Economics, Economics Discussion Papers 594, Apr. 2005. [Online]. Available: <http://ideas.repec.org/p/esx/essedp/594.html>
- [2] K. Ramadas and R. Jain, “WiMAX System Evaluation Methodology,” Wimax Forum, Jan 2007.
- [3] “WiMAX Forum Mobile System Profile 4 Release 1.0 Approved Specification,” Wimax Forum, May 2007.
- [4] G. Nogueira, B. Baynat, M. Maqbool, and M. Coupechoux, *Performance Evaluation and Dimensioning of WiMAX*. Book Chapter in “WiMAX Networks Planning and Optimization”, Auerbach Publications, CRC Press, Taylor & Francis Group, 2008.
- [5] B. Baynat, S. Doirieux, G. Nogueira, M. Maqbool, and M. Coupechoux, “An Efficient Analytical Model for WiMAX Networks with Multiple Traffic Profiles,” in *Proc. of ACM/IET/ICST IWPAWN*, Sep 2008.
- [6] D. Huo, “Clarification on the wrap-around hexagon network structure,” IEEE 802.20 Working Group on Mobile Broadband Wireless Access, IEEE C802.20-05/15, March 2005.
- [7] J. Khun-Jush, “Cdma uplink power control methodology in seamcat (voice only),” SEAMCAT Technical Group, STG(03)13 r1, October 2003.
- [8] D. Sinha, H. Zhou, and N. V. Shenoy, “Advances in Computation of the Maximum of a Set of Gaussian Random Variables,” in *Trans. of IEEE on Computer-Aided Design of Integrated Circuits and Systems*, Aug 2007.
- [9] M. Maqbool, M. Coupechoux, and P. Godlewski, “Comparative Study of Reuse Patterns for WiMAX Cellular Networks,” TELECOM ParisTech, Technical Report, 2008.

- [10] M. Maqbool, M. Coupechoux and P. Godlewski, “Comparison of Various Frequency Reuse Patterns for WiMAX Networks with Adaptive Beamforming,” in *Proc. of IEEE VTC Spring*, May 2008.